

## Stress-stress correlator in $\phi^4$ theory: Poles or a Cut?

---

**Guy D. Moore**

*Institut für Kernphysik, Technische Universität Darmstadt  
Schlossgartenstraße 2, D-64289 Darmstadt, Germany*

*E-mail:* [guy.moore@physik.tu-darmstadt.de](mailto:guy.moore@physik.tu-darmstadt.de)

**ABSTRACT:** We explore the analytical properties of the traceless stress tensor 2-point function at zero momentum and small frequency (relevant for shear viscosity and hydrodynamic response) in hot, weakly coupled  $\lambda\phi^4$  theory. We show that, rather than one or a small number of poles, the correlator has a cut along the negative imaginary frequency axis. We briefly discuss this result's relevance for constructing 2'nd order hydrodynamic models of hot relativistic field theories.

**KEYWORDS:** Transport, kinetic theory, shear viscosity, hydrodynamics

---

## Contents

<b>1</b>	<b>Introduction</b>	<b>1</b>
<b>2</b>	<b>Calculation ingredients</b>	<b>4</b>
2.1	Retarded and symmetrized correlators	4
2.2	Kinetic theory setup	5
2.3	Variational solution	7
<b>3</b>	<b>Discrete approximations to continuous spectra</b>	<b>9</b>
3.1	Example: Padé approximation	9
3.2	Application: shear correlator	11
<b>4</b>	<b>Discussion</b>	<b>14</b>

---

## 1 Introduction

Relativistic hydrodynamics is the universal effective theory for describing relativistic fluids which vary on sufficiently long time and length scales that they remain locally near equilibrium (even if the temperature, velocity, and any chemical potentials vary by a large amount on long scales, for a comprehensive recent review see [1]). For real-world applications it is important to include the effects of small departures from local equilibrium, arising from the fluid’s nonuniformity, see [2] for a review. Often this disequilibrium is controlled primarily by the shear viscosity  $\eta$ . But a *relativistic* hydrodynamic theory containing only shear viscosity suffers from instability and acausality problems [3–5], and must be supplemented with additional, higher-order corrections [6, 7]. Qualitatively these take the form of an exponential relaxation of the stress tensor towards a viscous-fluid form. They lead to a more complex hydrodynamic theory described by a larger number of coefficients.

There is an ongoing discussion on how to correctly interpret higher-order hydrodynamics. In the absence of conserved quantities besides energy and momentum, hydrodynamics is a theory to determine the evolution of the stress tensor  $T^{\mu\nu}$  from its equation of state,  $P = P(\varepsilon)$  with  $P$  the pressure and  $\varepsilon$  the energy density (each in the local rest frame). Shear viscosity enters the first-order theory as a correction to the functional form of the stress tensor,<sup>1</sup>

$$T^{\mu\nu} = T_{\text{eq}}^{\mu\nu} + \Pi^{\mu\nu}, \quad T_{\text{eq}}^{\mu\nu} = (\varepsilon + P)u^\mu u^\nu + P g^{\mu\nu}, \quad (1.1)$$

$$\Pi_{\text{1-order}}^{ij} = -\eta \left( \partial^i u^j + \partial^j u^i - \frac{2}{3} \delta^{ij} \partial_k u^k \right) - \zeta \delta^{ij} \partial_k u^k, \quad (1.2)$$

---

<sup>1</sup>We are using  $[-+++]$  metric conventions.

where  $T^{\mu\nu}$  is the stress tensor,  $u^\mu$  is the flow 4-velocity in the Landau-Lifshitz frame ( $u_\mu \Pi^{\mu\nu} = 0$ ), and the expression for the first-order nonequilibrium stress  $\Pi_{1\text{-order}}^{\mu\nu}$  has been written for the local rest frame. The first-order theory consists of using  $\Pi_{1\text{-order}}^{ij}$  from Eq. (1.2) as  $\Pi^{ij}$  in Eq. (1.1). The expression shows that the 5  $\ell=2$  modes behave quite differently than the one  $\ell=0$  ( $\delta^{ij}$ ) mode, so we implicitly project out the  $\delta^{ij}$  component of  $T^{ij}$  to concentrate on the  $\ell = 2$  part in the following; that is, from now on, when we write  $T^{ij}$  we mean  $T^{ij} - \delta^{ij}T^{kk}/3$ .

Eq. (1.1) should be understood as an infrared effective description. But for numerical applications we need to reformulate Eq. (1.1) in a way which leads to stable evolution on all scales; the reformulation must reduce to  $\Pi^{ij} = \Pi_{1\text{-order}}^{ij}$  for slowly-varying systems, and if the reformulation leads to more accurate behavior that is an added benefit. Israel and Stewart proposed a now-standard second-order reformulation [6, 7], in which  $\Pi^{ij}$  is related to  $\Pi_{1\text{-order}}^{ij}$  through a relaxation process,

$$\tau_\pi \partial_t \Pi^{ij} = \Pi_{1\text{-order}}^{ij} - \Pi^{ij}. \quad (1.3)$$

This introduces a new coefficient  $\tau_\pi$ . In one interpretation, this coefficient should be chosen in order to optimize the accuracy of  $\Pi^{ij}$  in a slowly varying system. That is, the transport coefficient  $\tau_\pi$ , and others which appear at this order in derivatives, should be chosen so as to optimally describe the behavior of hydrodynamic systems which vary slowly in space and time. This approach is implicit for instance by Baier *et al* [8] (see also [9]), who use it to derive a Kubo relation for this coefficient, which is then evaluated in a strongly coupled holographic theory [8].

Alternatively, we can interpret Eq. (1.3) as an attempt to really describe the microscopic physics by which the off-equilibrium stress tensor  $\Pi^{ij}$  approaches its near-equilibrium form  $\Pi_{1\text{-order}}^{ij}$ . In equilibrium in the absence of flow such that  $\Pi_{1\text{-order}}^{ij} = 0$ , the initial  $\Pi^{ij}(t=0)$  can be interpreted as that due to random thermal fluctuations, and the equation then gives a specific prediction for the stress tensor autocorrelator. Eq. (1.3) amounts to an *Ansatz* that the two-point correlator is controlled by a retarded function with a single pole<sup>2</sup> with imaginary part  $-i/\tau_\pi$ ,

$$\begin{aligned} \int d^3x \langle \Pi^{ij}(x,t) \Pi^{ij}(0,0) \rangle &= e^{-|t|/\tau_\pi} \int d^3x \langle \Pi^{ij}(x,0) \Pi^{ij}(0,0) \rangle \Rightarrow \\ G_s^{\pi\pi}(\omega) &\equiv \int e^{i\omega t} \langle \Pi^{ij}(x,t) \Pi^{ij}(0,0) \rangle d^3x dt \\ &= 10T \frac{4P}{5} \int e^{i\omega t} e^{-|t|/\tau} dt = 8PT \frac{2\tau_\pi^{-1}}{\omega^2 + \tau_\pi^{-2}}. \end{aligned} \quad (1.4)$$

Here 10 is the number of  $\ell = 2$  components appearing in the sum in  $T^{ij}T^{ij}$  and  $4PT/5$  is the equal-time, mean-squared fluctuation in each component in our kinetic description.<sup>3</sup> This is exactly the behavior of the correlator in the so-called relaxation-time approximation.

<sup>2</sup>Eq. (1.4) doesn't have a single pole; it has two poles, at  $\omega = \pm i\tau_\pi^{-1}$ . That is because it is the symmetrized correlator, not the retarded one; we will explain the relation shortly.

<sup>3</sup>The number of terms is 10 because there are  $2\ell + 1 = 5$  independent terms which are each double-counted in the sum, for instance,  $T^{xy} = T^{yx}$  is one of the 5 terms but both  $T^{xy}T^{xy}$  and  $T^{yx}T^{yx}$  appear in the sum. The equal-time correlator  $\int d^3x \langle \Pi^{xy}(x,0) \Pi^{xy}(0,0) \rangle$  equals the  $\omega$ -integral of  $G_s^{\pi\pi}(\omega)/10$  and

Denicol and collaborators have argued [10] that we can use a slightly modified form of Eq. (1.3) to improve the behavior of a slowly varying system *and* to simulate with maximal fidelity the microscopic behavior, by replacing Eq. (1.3) with

$$\tau_{\pi,\text{micro}} \partial_t \Pi^{ij} = -\Pi^{ij} + \left( \Pi_{1\text{-order}}^{ij} + (\tau_{\pi,\text{micro}} - \tau_{\pi,\text{macro}}) \partial_t \Pi_{1\text{-order}}^{ij} \right), \quad (1.5)$$

where  $\tau_{\pi,\text{macro}}$  is the definition in terms of slowly varying systems and Kubo relations, and  $\tau_{\pi,\text{micro}}$  is the imaginary part of the pole in  $G_s^{\pi\pi}(\omega)$  closest to the real axis. This definition assumes (as noted in [10]) that the stress tensor Green function has such a pole, rather than a cut structure. This appears to be a reasonable assumption. For instance it is consistent with the behavior obtained in strongly-coupled analogue theories with holographic duals, such as  $\mathcal{N}=4$  SYM theory at strong coupling with many colors. In this case we know that the dual theory contains a black hole, and the relevant correlator shows exponential decay, characterized by several complex exponents determined by the quasinormal modes of this dual black hole [11]. Note however that the behavior of such analogue theories at finite coupling, where known, is generally more complex [12]; the poles with  $\text{Re}\omega \neq 0$  move towards the real axis, and new poles appear on the imaginary axis and move towards the origin.<sup>4</sup> The relaxation-time approximation, which is often considered for simplicity and has sometimes been advocated on theoretical grounds [13, 14], corresponds to the presence of exactly one pole in the lower half-plane.

But it is by no means obvious that  $G_s^{\pi\pi}$  really is controlled by one or a small number of poles. It would be useful to know the behavior of more theories to see whether they contain poles, like SYM theory, or cuts. In this paper we address this for weakly coupled scalar  $\lambda\phi^4$  theory. We do so because the interactions are simple enough to allow an extremely precise study within kinetic theory, which is the relevant effective description for small self-coupling  $\lambda$ . We expect this theory to be representative of the behavior of weakly coupled QCD. If we see behavior substantially different than in SYM theory, it raises interesting questions about whether the analytic behavior of the 2-point function really is controlled by poles.

The question we address bears some similarity to the topic of two recent studies, one by Romatschke [15] and one by Kurkela and Wiedemann [16]. However the emphasis is somewhat different. These references wanted to study the wave-number  $k$  dependence of stress-stress correlation functions, including those which contain hydrodynamic poles, whereas we will look only at the  $k = 0$  limit and we concentrate on a correlator which determines a hydrodynamic coefficient but does not itself possess hydrodynamic poles. Because of their broader subject, the other studies made simplifying assumptions about scattering (relaxation-time approximations), whereas the point of our study is precisely to avoid this and to consider the full structure of scattering in a specific theory. We will return to this issue when we present our main results. Both sets of studies are relevant in comparing

---

should equal  $PT$ . At weak coupling,  $4/5$  of this contribution arises from very small frequencies which are accounted for in this kinetic theory calculation, and  $1/5$  arises from cut-type structures at frequencies  $\omega \sim T$ . Hence the factor  $4/5$  in our expression.

<sup>4</sup>Note that the  $\langle T^{ij}T^{ij} \rangle$  correlator is called the scalar channel in the holography community; they reserve “shear channel” to describe  $\langle T^{0i}T^{0i} \rangle(k)$  with  $i$  unsummed and orthogonal to spatial  $\mathbf{k}$ .

between weak-coupling behavior and the structure of poles observed at strong coupling [11], but our main motivation lies in the interpretation of second-order hydrodynamics as explained above. We therefore consider the studies by Romatschke and by Kurkela and Wiedemann to be complementary to ours.

In the next section we develop the tools to study the spectral properties within kinetic theory approximately. The approximate procedure we have available always results in a  $G_s^{\pi\pi}(\omega)$  which is a rational function; therefore it is similar to the problem of fitting analytic functions with a Padé approximant. So we will also give a quick sketch of what functions with poles, and with cuts, look like when we try to fit them using rational functions. Finally we will present our results and argue that they indicate the spectral function to have a cut, rather than a series of well-separated (quasinormal mode) poles. However, we will show that the cut carries most of its spectral weight over a relatively narrow range of frequencies.

## 2 Calculation ingredients

Here we review the tools which we will use to study the analytic property of the  $G_s^{\pi\pi}$  correlator in weakly-coupled theories via kinetic theory. We begin by reminding the reader of the relation between retarded and symmetrized correlation functions. Then we show how the symmetrized correlation function is evaluated in kinetic theory, and how kinetic theory is solved as a variational problem.

### 2.1 Retarded and symmetrized correlators

The Kubo relation for the shear viscosity is most naturally derived in terms of the retarded correlation function of the stress tensor,

$$\eta = \frac{1}{10} \lim_{\omega \rightarrow 0} \frac{1}{\omega} \text{Im} \int d^4x e^{i\omega t} G_R^{\pi\pi}(x, t), \quad (2.1)$$

$$G_R^{\pi\pi}(x, t) \equiv i \left\langle \left[ \Pi^{ij}(x, t), \Pi^{ij}(0, 0) \right] \right\rangle \Theta(t). \quad (2.2)$$

Because of the  $\Theta(t)$  factor, the retarded correlator  $G_R^{\pi\pi}(\omega)$  is nonsingular for frequencies with nonnegative imaginary part and has its singularities strictly in the lower frequency half-plane. It has a KMS relation with the symmetrized correlator

$$G_s^{\pi\pi}(\omega) = \frac{e^{\omega/T} + 1}{2(e^{\omega/T} - 1)} \text{Im} G_R^{\pi\pi}(\omega) \simeq \frac{T}{\omega} \text{Im} G_R^{\pi\pi}(\omega), \quad (2.3)$$

where in the second step we have made a small- $\omega$  approximation, which is appropriate at weak coupling where the relevant frequencies will be suppressed by powers of the coupling  $\omega \sim \lambda^2 T$ . Using this relation, a simple pole in the retarded function corresponds to a pair of poles in the symmetrized correlation function:

$$G_R^{\pi\pi}(\omega) = \dots + \frac{C}{\Gamma - i\omega} \quad \Rightarrow \quad G_s^{\pi\pi}(\omega) = \dots + \frac{CT}{(\Gamma + i\omega)(\Gamma - i\omega)}. \quad (2.4)$$

Though it is not our emphasis in this work, we remark that the KMS relation lets us express the viscosity in terms of  $G_s^{\pi\pi}$ :

$$\eta = \frac{1}{10T} \lim_{\omega \rightarrow 0} \int d^4x e^{i\omega t} G_s^{\pi\pi}(x, t) = \frac{1}{10T} \int d^4x G_s^{\pi\pi}(x, t). \quad (2.5)$$

Within kinetic theory, the stress tensor is expressed in terms of the statistical function  $f(p, x, t)$  as

$$T^{ij}(x, t) = \int \frac{d^3p}{(2\pi)^3} \frac{p^i p^j}{E_p} f(p, x, t), \quad E_p \equiv \sqrt{p^2 + m^2}. \quad (2.6)$$

(In a multicomponent or multiparticle theory we should add an index for particle type, which is summed over. We will leave this out as we will eventually specialize to a one-component scalar.) For the  $\ell = 2$  components of the stress tensor, the angular average above gives zero if we evaluate it using the equilibrium values of  $f$ ,  $f_0 = (\exp(-E_p/T) \mp 1)^{-1}$  for a system at rest at temperature  $T$ . However the statistical functions possess fluctuations; the well-known Bose or Fermi number fluctuations are in this context

$$\langle f(p, x, 0) f(q, x', 0) \rangle = f_0(p) f_0(q) + (2\pi)^3 \delta^3(p - q) \delta^3(x - x') f_0(p) [1 \pm f_0(p)] \quad (2.7)$$

with  $\pm$  a  $+$  for bosons and a  $-$  for fermions, and with  $f_0(p)$  the equilibrium mean occupancy. Therefore

$$\int d^3x \langle \Pi^{ij}(x) \Pi^{ij}(0) \rangle = \int \frac{d^3p}{(2\pi)^3} \frac{p^i p^j - \frac{\delta^{ij} p^2}{3}}{E} \frac{p^i p^j - \frac{\delta^{ij} p^2}{3}}{E} f_0(p) [1 \pm f_0(p)] = 10 \frac{4PT}{5} \quad (2.8)$$

with  $P, T$  the pressure and temperature as before. To determine the time structure of this correlation function, we need to establish the time dependence of the statistical function  $f(x, p, t)$ .

## 2.2 Kinetic theory setup

We consider scalar field theory with a single real field  $\phi$  with Lagrangian

$$-\mathcal{L}[\phi, \partial_\mu \phi] = \frac{1}{2} \partial_\mu \phi \partial^\mu \phi + \frac{m^2}{2} \phi^2 + \frac{\lambda}{24} \phi^4, \quad (2.9)$$

and in this work we consider  $m^2 \ll T^2$  so it can be neglected and we work perturbatively in  $\lambda$ . The scattering matrix element is precisely  $\mathcal{M} = \lambda$ , which will lead to simple momentum dependence in what follows.

At weak coupling and for the dominant  $p \sim \pi T$  modes which control thermodynamics and viscosity, we may make the quasiparticle approximation and apply kinetic theory. We will not review kinetic theory in detail, referring the reader for its derivation and application towards this problem to the literature [17–22]. The statistical function obeys a Boltzmann equation, which for our space-uniform system is of the form

$$\begin{aligned} \frac{\partial}{\partial t} f(\mathbf{p}, x, t) &= -\mathcal{C}[f] \\ \mathcal{C} &= \frac{1}{2} \frac{1}{2} \int \frac{d^3k d^3p' d^3k'}{(2\pi)^9 2k 2p' 2k'} (2\pi)^4 \delta^4(P+K-P'-K') |\mathcal{M}|^2 \\ &\quad \times \left( f(\mathbf{p}) f(\mathbf{k}) [1 \pm f(\mathbf{p}')] [1 \pm f(\mathbf{k}')] - f(\mathbf{p}') f(\mathbf{k}') [1 \pm f(\mathbf{p})] [1 \pm f(\mathbf{k})] \right), \end{aligned} \quad (2.10)$$

where the first line is the Boltzmann equation with  $\mathcal{C}$  the collision operator; the second line is the form of the collision operator for  $2 \leftrightarrow 2$  scattering; and the final line is the combination

of statistical functions showing removal and addition of a particle of momentum  $p$  (in which we have suppressed writing the dependence on  $(x, t)$ ). Capital letters are 4-vectors while lower case letters represent momenta or their magnitudes. The factor  $1/2$  in the first line of  $\mathcal{C}$  is a final-state symmetry factor. We are interested in the case where a  $t = 0$  initial fluctuation is of form (the factor  $\sqrt{3/2}$  is to follow the conventions of [21])

$$\delta f(\mathbf{p}, t = 0) = X_{ij} \sqrt{\frac{3}{2}} \frac{p^i p^j - \frac{\delta^{ij} p^2}{3}}{E} f_0(p) [1 \pm f_0(p)] \quad (2.11)$$

so that a specific component  $\Pi^{ij} \propto X^{ij}$  is nonzero; we then want to see how that fluctuation relaxes with time, so we can convert the equal-time correlator in Eq. (2.8) into an unequal time correlator and then into a frequency-domain correlator. Alternatively in the case that the fluid is under shear flow,  $X_{ij}$  represents the shear stress applied on the fluid [21]. The angular dependence is captured by writing  $\delta f(\mathbf{p}, t)$  with the *Ansatz*

$$\delta f(\mathbf{p}, t) = X_{ij} \chi_{ij}(\mathbf{p}, t) f_0(p) [1 \pm f_0(p)], \quad \chi_{ij}(\mathbf{p}, t) = \sqrt{3/2} (\hat{p}_i \hat{p}_j - \delta_{ij}/3) \chi(p, t). \quad (2.12)$$

The form of the *Ansatz* is ensured by the rotational symmetry of the theory and the fact that we work only to linear order in perturbations. To find the time evolution of  $\chi(p, t)$  we insert Eq. (2.12) in Eq. (2.10), finding after a little work [19]

$$\begin{aligned} -\frac{\partial \chi(p, t)}{\partial t} &= \mathcal{C}[\chi(p, t)] \\ &= \frac{\lambda^2}{2} \int \frac{d^3 k d^3 p' d^3 k'}{(2\pi)^9 2p 2p' 2k 2k'} (2\pi)^4 \delta^4(P+K-P'-K') f_0(p) f_0(k) [1+f_0(p')] [1+f_0(k')] \\ &\quad \times \left( \chi(p, t) + P_2(c_{pk}) \chi(k, t) - P_2(c_{pp'}) \chi(p', t) - P_2(c_{pk'}) \chi(k', t) \right). \end{aligned} \quad (2.13)$$

Here  $P_2(c_{pk})$  is the second Legendre polynomial with  $c_{pk} = \cos \hat{p} \cdot \hat{k} = \vec{p} \cdot \vec{k} / pk$ .

Formally, the space of possible  $\chi(p)$  form an infinite dimensional vector space  $\mathcal{L}^2$  (Lebesgue-square-integrable functions) with measure

$$\begin{aligned} \langle \chi_1(p) | \chi_2(p) \rangle &\equiv T^{-3} \int \frac{d^3 p}{(2\pi)^3} \chi_{ij1}(\mathbf{p}) \chi_{ij2}(\mathbf{p}) f_0(p) [1 \pm f_0(p)] \\ &= \frac{4\pi}{(2\pi T)^3} \int f_0(p) [1 \pm f_0(p)] \chi_1(p) \chi_2(p) p^2 dp \end{aligned} \quad (2.14)$$

and  $\mathcal{C}(\chi)$  acts as a positive symmetric operator on this space [21]. As such, it can be expressed in terms of its spectrum, which may contain both discrete and continuous components. Specifically, we can write the action of the collision operator in terms of eigenvalues and eigenvectors as

$$\mathcal{C} | \chi \rangle = \left( \sum_i \lambda_i | \xi_i \rangle \langle \xi_i | + \int d\lambda_j \lambda_j | \xi_j \rangle \langle \xi_j | \right) | \chi \rangle \quad (2.15)$$

with  $\lambda_i$  the discrete eigenvalues with eigenvectors  $| \xi_i \rangle$  and with the  $\int d\lambda_j$  integration running over any continuous spectrum the operator may possess. The eigenvectors are

orthonormal,  $\langle \xi_{i_1} | \xi_{i_2} \rangle = \delta_{i_1 i_2}$  and  $\langle \xi_{j_1} | \xi_{j_2} \rangle = \delta(j_1 - j_2)$  (Kroneker and Dirac delta functions).

In terms of this (in principle solvable) spectral decomposition, the departure at an arbitrary time is solved as

$$\chi(p, t) = \sum_i \langle \xi_i | \chi(p, 0) \rangle \xi_i(p) e^{-\lambda_i t} + \int d\lambda_j \langle \xi_j | \chi(p, 0) \rangle \xi_j(p) e^{-\lambda_j t}. \quad (2.16)$$

That is, the initial departure from equilibrium is decomposed in terms of the eigenvectors of the collision operator, which each decay exponentially at a rate controlled by the respective eigenvalue. The Boltzmann equation should only be used at positive times because it is structured in terms of a dissipative response to an initial condition, but by time symmetry the negative- $t$  correlators are the same as at positive  $t$ , and so the stress-stress correlator and the shear viscosity evaluate to

$$G_s^{\pi\pi}(\omega) = \sum_i \frac{2\lambda_i T^3}{\lambda_i^2 + \omega^2} |\langle \chi(p, 0) | \xi_i \rangle|^2 + \int d\lambda_j \frac{2\lambda_j T^3}{\lambda_j^2 + \omega^2} |\langle \chi(p, 0) | \xi_j \rangle|^2, \quad (2.17)$$

$$\eta = \frac{G_s^{\pi\pi}(0)}{10T} = \sum_i \frac{T^2}{5\lambda_i} |\langle \chi(p, 0) | \xi_i \rangle|^2 + \int d\lambda_j \frac{T^2}{5\lambda_j} |\langle \chi(p, 0) | \xi_j \rangle|^2. \quad (2.18)$$

This is then evaluated by treating the squared fluctuation  $|\chi(p, 0)\rangle\langle\chi(p, 0)|$  using Eq. (2.7). The eigenvalues of the discrete/continuous spectrum of the linearized collision operator  $\mathcal{C}$  correspond to locations of poles/cuts in the stress tensor Green function, with residue/discontinuity determined by the overlap of the associated eigenvector with the initial departure from equilibrium.

### 2.3 Variational solution

The collision operator is determined through its matrix elements. Using the definitions of the previous section, we have

$$\begin{aligned} \langle \chi_1 | \mathcal{C} | \chi_2 \rangle &= \int \frac{d^3 p d^3 k d^3 p' d^3 k'}{(2\pi)^{12} 2p 2k 2p' 2k'} (2\pi)^4 \delta^4(P+K-P'-K') |\mathcal{M}_{\mathbf{p}\mathbf{k}\mathbf{p}'\mathbf{k}'}|^2 \\ &\quad \times f_0(p) f_0(k) [1 \pm f_0(p')] [1 \pm f_0(k')] \times (\chi\text{-factor}), \end{aligned} \quad (2.19)$$

$$\begin{aligned} (\chi\text{-factor}) &= \frac{1}{2} \chi_{ij1}(\mathbf{p}) \left[ \chi_{ij2}(\mathbf{p}) + \chi_{ij2}(\mathbf{k}) - \chi_{ij2}(\mathbf{p}') - \chi_{ij2}(\mathbf{k}') \right] \\ &= \frac{1}{8} \left[ \chi_{ij1}(\mathbf{p}) + \chi_{ij1}(\mathbf{k}) - \chi_{ij1}(\mathbf{p}') - \chi_{ij1}(\mathbf{k}') \right] \left[ \chi_{ij2}(\mathbf{p}) + \chi_{ij2}(\mathbf{k}) - \chi_{ij2}(\mathbf{p}') - \chi_{ij2}(\mathbf{k}') \right]. \end{aligned} \quad (2.20)$$

Here we use the symmetry of the first two lines to symmetrize the  $\chi_1$  dependence of the first factor. To evaluate this we use repeatedly that

$$\chi_{ij1}(\mathbf{p}) \chi_{ij2}(\mathbf{k}) = P_2(c_{pk}) \chi_1(\mathbf{p}) \chi_2(\mathbf{k}). \quad (2.21)$$

Because  $|\mathcal{M}_{\mathbf{p}\mathbf{k}\mathbf{p}'\mathbf{k}'}|^2 = \lambda^2$ , we also use the ‘‘s-channel’’ integration variables [22]

$$\begin{aligned} \langle \chi_1 | \mathcal{C} | \chi_2 \rangle &= \frac{\lambda^2}{(4\pi)^6 T^3} \int_0^\infty d\omega \int_0^\omega dp \int_0^\omega dp' \int_{\omega-2\min[p,p',k,k']}^\omega dq \int_0^{2\pi} d\phi \\ &\quad \times f_0(p) f_0(k) [1 + f_0(p')] [1 + f_0(k')] \\ &\quad \times \left( \chi_1(p) \chi_2(p) P_2(c_{pp}) + \chi_1(p) \chi_2(k) P_2(c_{pk}) - \chi_1(p) \chi_2(p') P_2(c_{pp'}) + \dots \right), \end{aligned} \quad (2.22)$$

where the final line contains 16 total terms corresponding to each  $\chi_1$  and  $\chi_2$  argument ranging over  $(p, k, p', k')$ ; the sign is positive/negative for an even/odd number of primes (final-state particles). Here  $k, k'$  are

$$k = \omega - p, \quad k' = \omega - p', \quad (2.23)$$

the Mandelstam variables are

$$s = \omega^2 - q^2, \quad u = -s - t, \quad t = \frac{s}{2q^2} \left( (p-k)(p'-k') - q^2 + \cos \phi \sqrt{(4pk-s)(4p'k'-s)} \right), \quad (2.24)$$

and the cosines of angles are  $c_{pp} = 1 = c_{p'p'}$  and

$$\begin{aligned} c_{pk} &= 1 - \frac{s}{2pk}, & c_{p'k'} &= 1 - \frac{s}{2p'k'}, & c_{pp'} &= 1 + \frac{t}{2pp'}, \\ c_{kk'} &= 1 + \frac{t}{2kk'}, & c_{pk'} &= 1 + \frac{u}{2pk'}, & c_{p'k} &= 1 + \frac{u}{2p'k}. \end{aligned} \quad (2.25)$$

The  $\phi$  integral is trivial and the  $q$  integral can be performed as well because no statistical or  $\chi$ -function depends on it. However we are only able to accomplish the remaining integrals numerically even if the forms of  $\chi_1$  and  $\chi_2$  are known. For this reason, to date we have not been able to explicitly solve the eigenvalue/eigenvector decomposition of  $\mathcal{C}$  without further approximation. Note that so far our only approximation has been the small  $\lambda$  expansion.

At this point we abandon an exact eigenvalue/eigenvector decomposition of  $\mathcal{C}[\chi]$  and attempt such a decomposition only within a restricted eigenspace, by requiring  $\chi(p)$  to lie within a linear *Ansatz*. This is equivalent to replacing the full Hilbert space  $\mathcal{L}^2$  with the Hilbert subspace spanned by the chosen *Ansatz* eigenfunctions. For a well chosen and flexible basis of functions, this will typically capture the most important functions in the sense of those which dominate Eq. (2.17). Relevant properties should converge as we enlarge the considered basis, just as the low-lying eigenvalues become more accurate as one uses the same procedure to find the spectrum within the variational approach to quantum mechanics. But there are limitations when  $\mathcal{C}$  has a continuous spectrum, which we will address in the next section.

We choose the following variational form:

$$\chi(p) = \sum_{i=1}^M c_i \varphi_i(p), \quad \varphi_i(p) \equiv \frac{p^{i+1} T^{N-i-1}}{(p+p_0)^{N-1}}, \quad (2.26)$$

where  $p_0$  is an energy scale and  $M, N$  are integers which control the size and form of the basis. This is the same *Ansatz* used in [19, 21] except that we don't restrict either to  $p_0 = T$  or to  $M = N$ . It spans rational functions with  $(p+p_0)^{N-1}$  denominator, which flexibly accommodates functional forms with structure between about  $p_0/N$  to  $Np_0$ . The most IR behavior is restricted to be  $p^2$  because the collision integral grows rapidly with small  $p$  so that this functional dependence almost always occurs. We can determine how flexible the *Ansatz* is by picking  $M$ , with larger values giving a more flexible functional form. We can vary *where* this flexibility occurs by varying  $p_0$ , with larger values saving

more of the functional freedom for larger  $p$  values. And we can allow functions with stronger UV behavior by allowing  $M > N$ . The basis of  $\varphi_i(p)$  functions is not orthonormal but we make it so by applying the Gram-Schmidt process using the inner product given in Eq. (2.14). We then evaluate the matrix form of  $\mathcal{C}[\chi]$  by performing the integrals in Eq. (2.22) by numerical quadratures. We are able to get stable and precise matrix elements and eigenvector decomposition for up to 20 basis elements. As a cross-check, we use Eq. (2.18) to evaluate  $\eta$  for comparison with previous accurate evaluations. Checking for convergence with basis size and quadratures integration refinement, we find

$$\eta = 3033.5425 \frac{T^3}{\lambda^2}, \quad (2.27)$$

which compares well with 3040 found in [19] and 3033.54 found in [23].

### 3 Discrete approximations to continuous spectra

There is a problem with our procedure. When we restrict to a finite-element *Ansatz*, or equivalently we work within a finite-dimensional subspace of the infinite-dimensional  $\mathcal{L}^2$  space of  $\chi(p)$  functions, we automatically modify the possible form of the collision operator's spectrum. This is familiar from quantum mechanics. In a finite-dimensional Hilbert space, Hermitian (for us, real symmetric) operators automatically have a discrete spectrum. But in infinite-dimensional (but separable) Hilbert spaces, Hermitian operators generically have both discrete and continuous spectra<sup>5</sup>. The spectrum we find should go over to the infinite-dimensional spectrum in the limit that we enlarge our basis without limit. But how does a discrete spectrum turn into a continuous one, and how does one recognize whether that is what is happening?

#### 3.1 Example: Padé approximation

For this purpose we find it useful to look at another example. Consider analytical functions, which can have poles, zeros, and cuts. The process of approximating  $\mathcal{C}$  with a finite-dimensional Hilbert space is similar to rational approximations of analytical functions; a rational function has only a finite number of potential poles and zeros and cannot possess a cut. But in the limit that we take a rational approximation with more and more terms, it should converge to the underlying analytical function, with its cut structure. Therefore we will make an aside to explore how this looks in a few examples, and how one identifies what is converging to a pole and what to a cut in the high-order limit.

Consider first the function  $\ln(1+x)$ . It is terribly fit by its Taylor series for  $|x| > 1$  because a Taylor series fits an analytical function with a function possessing zeros but no poles. The logarithm function has a cut from  $-1$  to  $-\infty$ , and a cut is better fit by a nearly-equal number of zeros and poles. Therefore it would be better to approximate the function with an  $(M, N)$  Padé approximant with  $M = N$  or  $M = N + 1$ . We can make the

---

<sup>5</sup>Technically in generality self-adjoint operators can have pure-point, singular, and absolutely continuous spectrum [24].

Padé approximant unique by forcing the first  $M + N$  terms in its Taylor series to match the Taylor series of the logarithm function, resulting in

$$P_{11}(x) = \frac{1 + \frac{3}{2}x}{1 + \frac{1}{2}x}, \quad P_{22}(x) = \frac{1 + 2x + \frac{2}{3}x^2}{1 + x + \frac{1}{6}x^2}, \quad P_{33}(x) = \frac{1 + \frac{5}{2}x + \frac{8}{5}x^2 + \frac{7}{30}x^3}{1 + \frac{3}{2}x + \frac{3}{5}x^2 + \frac{1}{20}x^3}, \dots \quad (3.1)$$

The zeros/poles of each Padé approximant correspond to the zeros of the polynomial in the numerator/denominator.

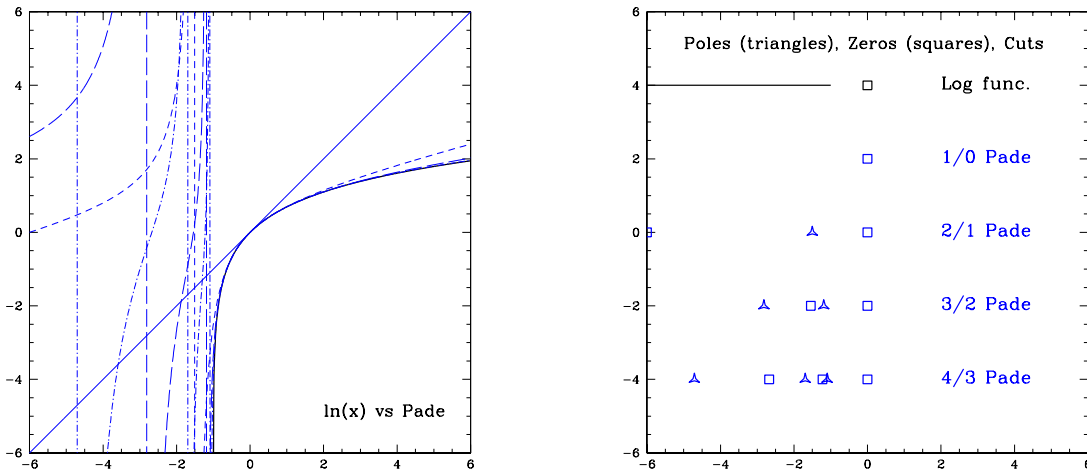


**Figure 1.** Fitting the logarithm function  $\ln(1+x)$  with Padé. Left: comparing the log function to the (1,0), (2,1), (3,2), and (4,3) Padé approximants. The higher approximants do an excellent job above  $x = -1$  and have a series of poles and zeros where the logarithm has its cut. Right: the location of zeros and poles of the Padé approximants, compared to the zero and cut of  $\ln(1+x)$ .

Figure 1 shows that such Padé approximants (the figure considers  $(M+1, M)$  approximants) work very well near  $x = 0$  (over a much wider range than the Taylor series, not shown), but “go crazy” where  $\ln(1+x)$  has its cut. Since the Padé function cannot have a cut, it instead has an alternating series of zeros and poles. As one uses more terms to get a better approximant, the poles and cuts get closer together and also cover more of the cut. If we could take the limit of a large order  $M$  of the Padé approximant, we would see the zeros and poles always alternating but getting closer and closer together and filling more and more of the negative axis.

We can also distinguish a pole from a cut in a function which has both; Figure 2 shows a similar study of the function  $f = \sqrt{(x+2)(x+3)/6}/(x+1)$ , which has a pole at  $x = -1$  and a cut from  $x = -2$  to  $x = -3$ . The Padé approximants fit the function well everywhere but in the cut, and the cut is easily identified as a region where alternating zeros and poles get denser and denser. The leading pole is fit very accurately, for essentially the same reason that the variational method is so good at establishing the ground state energy in quantum mechanics. We also studied a function with a series of poles, though we do not provide a figure. In this case, the Padé approximant comes close to capturing the first few poles but misses those which are farther away. This is again similar to how a

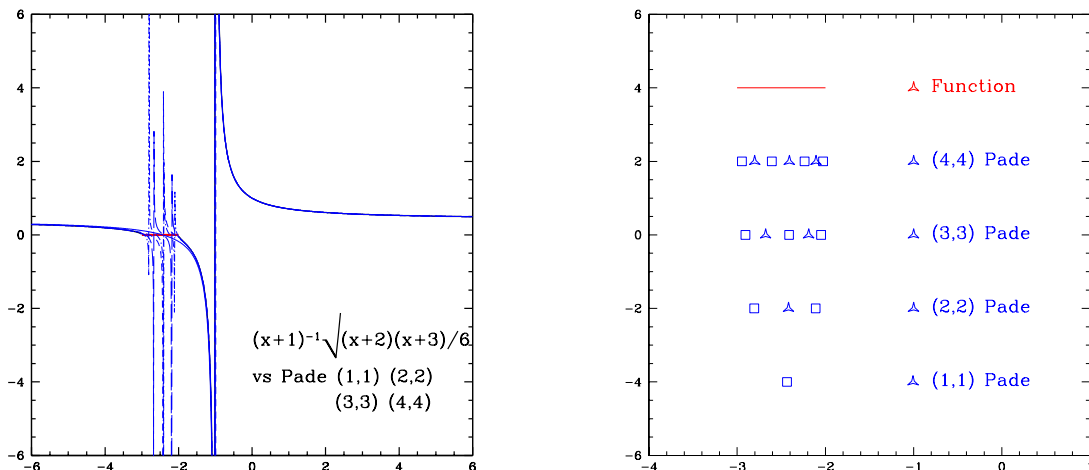


**Figure 2.** Padé fits (left) and poles/zeros (right) for the function  $\sqrt{(x+2)(x+3)}/6/(x+1)$ , which has a pole and a cut.

multi-parameter variational solution finds the first few energy levels of a quantum system but does a poor job with higher states.

### 3.2 Application: shear correlator

With this in mind, we present our results for the locations of poles in the stress-stress correlator. Rather than plot the locations of poles and of zeros, which continue to interleave, we plot only the locations of poles, but we plot them against each eigenvector's contribution to the shear viscosity as found in Eq. (2.18) – that is, in each plot we use as the  $y$ -axis the value  $\frac{T^2}{5\lambda_i} |\langle \chi(p, 0) | \xi_i \rangle|^2$  which the eigenvalue contributes to the shear viscosity or equivalently the residue of the pole in the viscosity correlator.

We start in Figure 3 by showing the dependence of the pole location and shear-contribution on the size of the variational basis. Each of the four panels represents the choice  $p_0 = T$ , but we choose  $(M, N)$  (the size of the basis and the power in the denominator) to be  $(4, 4)$ ,  $(10, 8)$ ,  $(16, 12)$ , and  $(20, 16)$ . As the figure shows, increasing the basis size leads to poles which cover a wider frequency range but are also denser, just as we found in the examples where a function with poles is approximating a cut. The functional form of Eq. (2.17) ensures that zeros interleave between these poles. The lowest pole also gets progressively lower with smaller residue, rather than becoming fixed, indicating that the first nonanalytic feature is not a pole but a branch point with very small initial discontinuity. (If the true behavior is a cut, then a large basis will have narrowly-spaced poles and the cut discontinuity will be the ratio of the pole residue to the inter-pole spacing.) Note that each figure is a log-log plot; the range of frequencies and of contributions to  $\eta$  are very large. The  $x, y$  axes are missing some units;  $\omega$  is measured in units of  $\lambda^2 T$  and  $\eta/s$  has a missing factor of  $1/\lambda^2$ .

If the spectrum contains poles and not a cut, one would also expect the locations of the more IR poles which contribute the most to  $\eta$  to be stable to changes in the basis

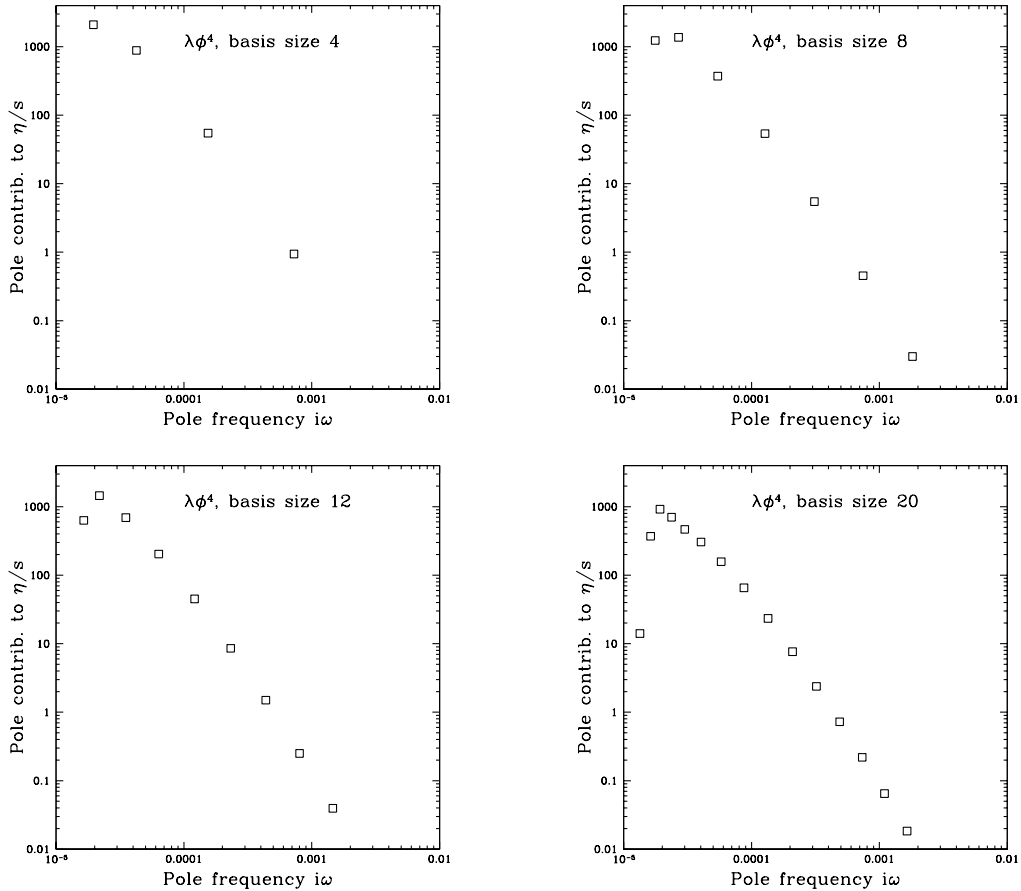


**Figure 3.** Location of poles, and contribution of each pole to  $\eta$ , for  $G_s^{\pi\pi}$  in  $\lambda\phi^4$  theory as a function of the size of the variational *Ansatz*. From top left to bottom right, the figures represent  $(M, N)$  of  $(4, 4)$ ,  $(10, 8)$ ,  $(16, 12)$ , and  $(20, 16)$ . With increasing basis size, the poles span a wider range but also draw closer together.

details. This is not the case, as shown in Figure 4. The figure shows what happens as we increase  $M$  at fixed  $N$ , which from Eq. (2.26) means that we are adding basis functions onto the UV end of the  $p$ -spectrum. Specifically, each pole set in the plot was found with a functional basis with  $N = 12$ , but  $M$  was increased from 12 to 14 to 16 while simultaneously changing  $p_0$  from 0.5 to 1 to 2. Therefore the functional basis became more sensitive to large- $p$  structure, but somewhat less sensitive to small- $p$  (IR) structure. As we shift from more IR to more UV sensitivity, the location of poles shifts, the poles get closer together (bringing down the individual contributions to  $\eta$  so that the sum stays the same), and the smallest  $\omega$  value observed gets smaller. (Note that 4, 3, and 2 poles lie off the high-frequency, small-residue side of the plot for the most IR, medium, and most UV sensitive basis, indicating that the most IR sensitive basis has more sensitivity at the high-frequency end.) This shows that the lowest- $\omega$  poles correspond to functional forms which lie mostly at large  $p$ , while the highest- $\omega$  poles lie mostly at small  $p$ . This behavior makes sense because the total scattering cross-section in  $\lambda\phi^4$  theory scales as  $1/s$  and therefore as

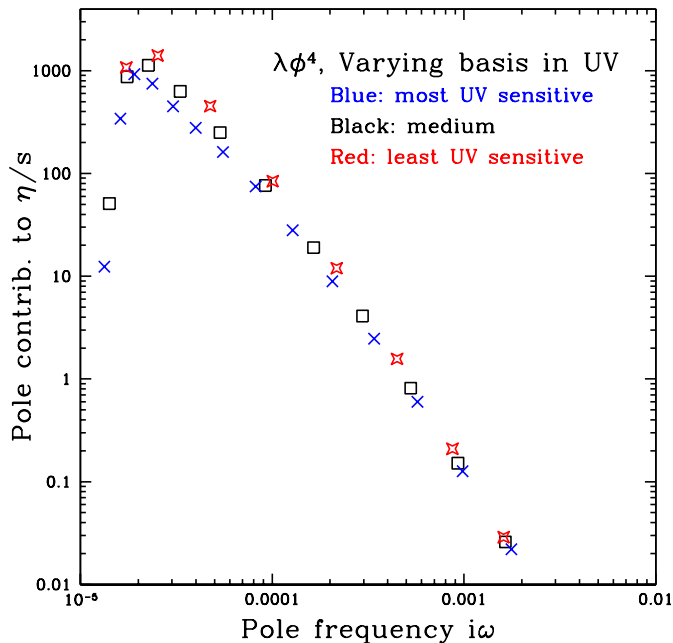


**Figure 4.** Pole locations for fixed  $N = 12$  and  $M = 12, 14, 16$ , with  $p_0 = 0.5, 1, 2$ . As basis functions are added at large  $p$  and the scale of sensitivity is shifted towards large  $p$ , pole locations move and the lowest observed frequency gets lower.

$1/p$ , indicating that high-energy particles live longer and low-energy particles change more quickly.

Finally it is useful to compare these results to what we would find in a simple-minded approximation for  $\mathcal{C}$  where we know the analytical structure. Consider then the generalized momentum-dependent relaxation-time approximation

$$\mathcal{C}[\chi(p)] = \tau^{-1}[p] \chi(p), \quad \tau[p] = \tau_0(T/p)^\alpha, \quad (3.2)$$

where  $\alpha$  controls the momentum dependence of the relaxation. The case  $\alpha = 0$  is the traditional relaxation-time approximation, in which all excitations approach equilibrium with the same speed. The choice  $\alpha = -1$  or  $\tau \propto p$  means that UV excitations relax more slowly than IR ones. This is the closest one can come to the real behavior of  $\lambda\phi^4$  theory within this family of approximations. Recently Kurkela and Wiedemann have explored the analytic structure of the  $\langle T^{0i}T^{0i} \rangle(k)$  (shear-channel) correlator as a function of  $k$  in this approximation [16], in a study complementary to ours. Romatschke's similar study [15] considers only  $\alpha = 0$ , so  $\tau = \tau_0$  independent of  $p$ .

Within this simplified approximation, the collision operator  $\mathcal{C}[\chi(p)]$  is diagonal in the  $p$ -basis, so the eigenvectors are the functions  $\chi(p) \propto \delta(p - p_0)$ , indexed by  $p_0$ . For  $\alpha = 0$  the eigenvalues are  $\omega = 1/\tau_0$  for all  $p_0$ . This degenerate eigenspectrum means that we can choose one eigenvector with perfect projection against  $|\chi(p, 0)\rangle$ , leading to a spectrum with a single pole. For  $\alpha = -1$  the eigenvalues are  $\omega = T/(p_0\tau_0)$ , leading to a cut along the whole imaginary  $\omega$  axis. Since small  $\omega$  corresponds to large  $p_0$ , the cut has exponentially

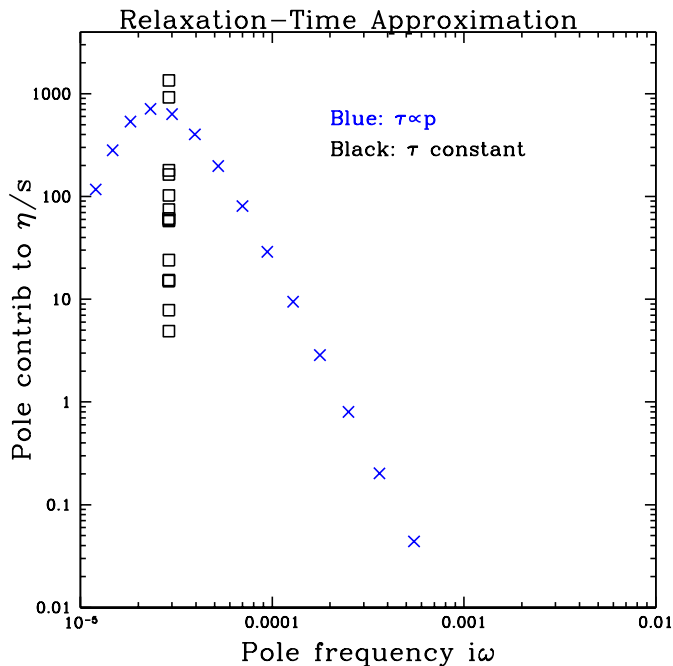


**Figure 5.** Pole locations when we apply the variational *Ansatz* method to the collision operator  $\mathcal{C}$  in the relaxation-time approximation, with a fixed relaxation time or with  $\tau \propto p$  (each scaled to give the same  $\eta$  result as the full case).

small discontinuity for small  $\omega$ ; whereas for large  $\omega$  and therefore small  $p_0$ , the discontinuity decays as a power of  $\omega$ . We might expect a similar behavior in  $\lambda\phi^4$  theory because the total scattering cross-section scales as  $\sigma \sim 1/s \sim 1/p$ .

We can use this solvable case to test how our multi-parameter *Ansatz* method performs. The results are shown in Figure 5. In each case we have set the overall coefficient of  $\mathcal{C}$  to reproduce the same  $\eta$  value that we found in the complete treatment, so Figures 3, 4, and 5 are directly comparable.<sup>6</sup> The figure shows that the single relaxation time indeed finds a single frequency. Our eigenvalue solver happened to pick a basis where the spectral weight was distributed over several modes, but since the modes are degenerate this is an arbitrary choice and we could change the basis to find a single pole. On the other hand, for the  $p$ -dependent relaxation-time approximation we find a series of poles which look quite similar to the behavior found for the true collision operator. That is, when we consider two toy collision operators, one with a pure-point spectrum and one with a continuous spectrum, the actual behavior of  $\lambda\phi^4$  closely resembles the continuous-spectrum toy model when we view each using the *Ansatz* method.

## 4 Discussion

The correlator of the trace-subtracted stress tensor plays a central role in hydrodynamics, controlling both the shear viscosity and certain “second-order” transport coefficients. If

<sup>6</sup>To make Figure 5 we used  $N = 16$  and  $M = 20$  with  $p_0 = T$ .

hydrodynamics is to be extended from describing slowly-varying systems near local equilibrium to more accurately reflecting microscopic relaxation processes (something we can hope for in second-order hydro), then we need to understand the analytical structure of  $G_s^{\pi\pi}(\omega)$  as accurately as possible.

Does  $G_s^{\pi\pi}(\omega)$  feature poles, as in strongly-coupled theories with holographic duals and in the simplest relaxation-time approximation? Or does it feature a cut or more complex analytic structure? We explored this question in a weakly-coupled theory,  $\lambda\phi^4$  theory. Within the kinetic-theory approximation (which should describe most weakly-coupled theories), the correlator has its nonanalyticities strictly on the negative imaginary-frequency axis. And in  $\lambda\phi^4$  theory, the nonanalyticity appears to be a cut. The evidence for a cut is that when we render the problem solvable, by restricting to a finite-dimensional (but large) subspace of departures from equilibrium, we find a dense set of poles which grow denser as the subspace is expanded. This behavior is typical for an approximation which must find poles, used on a function which in truth has a cut. It is also what we find in the  $p$ -dependent relaxation-time approximation, where we know there is a cut. And like the  $p$ -dependent relaxation-time approximation, we believe that the cut runs all the way up to  $\omega = 0$ , albeit with exponentially shrinking discontinuity.

We could attempt to make the same study for weakly coupled QCD. The collision integral is also known [22], but its more complicated form means that we cannot integrate it with enough precision to use really large bases of test functions. Therefore it is not so easy to see the limiting behavior as the basis is made large. However we anticipate the same qualitative behavior. In fact, since processes which exchange a small momentum have a large cross-section in gauge theories, we expect a much larger “tail” towards much higher frequencies within QCD, reflecting  $\chi(p)$  functions which oscillate rapidly as a function of  $p$ .

The most important conclusion of our work is that it is perfectly possible, indeed should perhaps be expected, that the stress-stress correlator  $G_s^{\pi\pi}(\omega)$  in real-world QCD has an analytic structure which is more complicated than a few well-isolated poles. Even if we knew this structure – for instance, if we assume that it is the same as in  $\lambda\phi^4$  theory – this precludes a second-order hydrodynamical treatment such as Eq. (1.5) from serving as a really accurate *microphysical* description of the relaxation process.

What we have *not* done is to study the behavior of the stress-tensor correlator at finite wave number  $k$ . To do so with the full nontrivial collision operator would require an extension of this work from departures from equilibrium with  $\ell = 2$  spherical-harmonic structure, to those with all  $\ell$  values. Such an approach would answer the question of how realistic collision integrals affect the conclusions of Romatschke’s [15] and Kurkela and Wiedemann’s [16] work. While technically feasible, such a study would be significantly more complicated, so we leave it for future work.

## Acknowledgments

We thank the Technische Universität Darmstadt and its Institut für Kernphysik, where this work was conducted. We also thank Rolf Baier and Andrei Starinets for inspiring us to

consider this problem, and to Paul Romatschke and Aleksi Kurkela for valuable discussions. The author acknowledges support by the Deutsche Forschungsgemeinschaft (DFG) through the grant CRC-TR 211 “Strong-interaction matter under extreme conditions.”

## References

- [1] Thomas Schäfer and Derek Teaney. Nearly Perfect Fluidity: From Cold Atomic Gases to Hot Quark Gluon Plasmas. *Rept. Prog. Phys.*, 72:126001, 2009.
- [2] Derek A. Teaney. Viscous Hydrodynamics and the Quark Gluon Plasma. In Rudolph C. Hwa and Xin-Nian Wang, editors, *Quark-gluon plasma 4*, pages 207–266. 2010.
- [3] Ingo Muller. Zum Paradoxon der Wärmeleitungstheorie. *Z. Phys.*, 198:329–344, 1967.
- [4] W. A. Hiscock and L. Lindblom. Stability and causality in dissipative relativistic fluids. *Annals Phys.*, 151:466–496, 1983.
- [5] William A. Hiscock and Lee Lindblom. Generic instabilities in first-order dissipative relativistic fluid theories. *Phys. Rev.*, D31:725–733, 1985.
- [6] W. Israel. Nonstationary irreversible thermodynamics: A Causal relativistic theory. *Annals Phys.*, 100:310–331, 1976.
- [7] W. Israel and J. M. Stewart. Transient relativistic thermodynamics and kinetic theory. *Annals Phys.*, 118:341–372, 1979.
- [8] Rudolf Baier, Paul Romatschke, Dam Thanh Son, Andrei O. Starinets, and Mikhail A. Stephanov. Relativistic viscous hydrodynamics, conformal invariance, and holography. *JHEP*, 04:100, 2008.
- [9] Sayantani Bhattacharyya, Veronika E Hubeny, Shiraz Minwalla, and Mukund Rangamani. Nonlinear Fluid Dynamics from Gravity. *JHEP*, 02:045, 2008.
- [10] Gabriel S. Denicol, Jorge Noronha, Harri Niemi, and Dirk H. Rischke. Origin of the Relaxation Time in Dissipative Fluid Dynamics. *Phys. Rev.*, D83:074019, 2011.
- [11] Pavel K. Kovtun and Andrei O. Starinets. Quasinormal modes and holography. *Phys. Rev.*, D72:086009, 2005.
- [12] Sao Grozdanov, Nikolaos Kaplis, and Andrei O. Starinets. From strong to weak coupling in holographic models of thermalization. *JHEP*, 07:151, 2016.
- [13] T. Koide, E. Nakano, and T. Kodama. Shear viscosity coefficient and relaxation time of causal dissipative hydrodynamics in QCD. *Phys. Rev. Lett.*, 103:052301, 2009.
- [14] T. Koide and T. Kodama. Transport Coefficients of Non-Newtonian Fluid and Causal Dissipative Hydrodynamics. *Phys. Rev.*, E78:051107, 2008.
- [15] Paul Romatschke. Retarded correlators in kinetic theory: branch cuts, poles and hydrodynamic onset transitions. *Eur. Phys. J.*, C76(6):352, 2016.
- [16] Aleksi Kurkela and Urs Achim Wiedemann. Analytic structure of nonhydrodynamic modes in kinetic theory. 2017.
- [17] L.P. Kadanoff and G. Baym. *Quantum statistical mechanics: Green’s function methods in equilibrium and nonequilibrium problems*. Frontiers in physics. W.A. Benjamin, 1962.
- [18] Sangyong Jeon. Hydrodynamic transport coefficients in relativistic scalar field theory. *Phys. Rev.*, D52:3591–3642, 1995.

- [19] Sangyong Jeon and Laurence G. Yaffe. From quantum field theory to hydrodynamics: Transport coefficients and effective kinetic theory. *Phys. Rev.*, D53:5799–5809, 1996.
- [20] Peter Brockway Arnold, Dam T. Son, and Laurence G. Yaffe. Effective dynamics of hot, soft nonAbelian gauge fields. Color conductivity and  $\log(1/\alpha)$  effects. *Phys. Rev.*, D59:105020, 1999.
- [21] Peter Brockway Arnold, Guy D. Moore, and Laurence G. Yaffe. Transport coefficients in high temperature gauge theories. 1. Leading log results. *JHEP*, 11:001, 2000.
- [22] Peter Brockway Arnold, Guy D Moore, and Laurence G. Yaffe. Transport coefficients in high temperature gauge theories. 2. Beyond leading log. *JHEP*, 05:051, 2003.
- [23] Guy D. Moore. Next-to-Leading Order Shear Viscosity in  $\lambda \phi^4$  Theory. *Phys. Rev.*, D76:107702, 2007.
- [24] M. Reed and B. Simon. *Methods of Modern Mathematical Physics. 1. Functional Analysis.* Academic Press, 1972.